

Hybrid Neem–Peepal Fiber Epoxy Composites Reinforced with Silica Nanoparticles: Toward Moisture-Resistant and Sustainable Bio-Based Materials

R. Kumar^{1, *}, M. Muthukumaran², J. Bensam Raj³

¹Department of Robotics and Automation, Dhaanish Ahmed Institute of Technology, Coimbatore, Tamil Nadu, Pin code - 641105, India

²Department of Mechanical Engineering, Jansons Institute of Technology, Coimbatore, Tamil Nadu, Pin code - 641659, India

³Department of Mechanical Engineering, Muthayammal Engineering College (Autonomous), Rasipuram, Tamil Nadu, Pin code - 637408, India

*Corresponding author: kumarsangili2015@gmail.com

Graphical abstract



Abstract

In light of the growing amount of urban green waste and the increasing demand for sustainable materials, it is clear that more needs to be done to repurpose biodegradable biomass into high-performance composites. This study valorized waste fibers from Peepal (*Ficus religiosa*) and Neem (*Azadirachta indica*) trees, commonly discarded during municipal pruning as reinforcements in epoxy composites. Adding of silica (SiO_2) nanoparticles further improved the mechanical and environmental durability of the materials. The composites were

fabricated using different stacking sequences (N/P/N and P/N/P) and SiO₂ nanoparticle loadings (1–3 wt%) and were then evaluated in term of their tensile strength, flexural strength, impact strength, surface hardness, and water absorption. The N/P/N configuration with 2 wt% SiO₂ exhibited the best performance, achieving a tensile strength of 70 MPa, flexural strength of 74 MPa, impact strength of 5.0 kJ/m², and surface hardness of 70 Shore D, while water absorption decreased to 52% with 3 wt% SiO₂, indicating enhanced moisture resistance. Improved density and reduced void content also validated the microstructural integrity. These results demonstrate the potential of hybrid bio-waste fiber and nano-reinforced epoxy composites as environmentally sustainable alternatives for structural and packaging applications.

Keywords:

Biowaste utilization; Hybrid epoxy materials; Mechanical characterization; Natural fiber composites; Silica nanoparticles reinforcement; Sustainable solid waste management

1. Introduction

Environmental degradation, the depletion of non-renewable resources, and the growing volume of synthetic polymer waste have driven the demand for sustainable material alternatives. Bio-composites, composed of natural fibers and biodegradable or recyclable polymer matrices, have emerged as promising replacements for conventional synthetic composites. Plant-derived fibers from agricultural and biomass waste are particularly attractive due to their low cost, renewability, and environmental benefits (Prasad et al. 2024; Santhosh et al. 2024)..

Valorizing agricultural residues through composite fabrication is a growing trend in sustainable materials engineering. For instance, Şen et al. (2025) developed PLA composites

with 1–10 wt% artichoke stem particles (AP), improving stiffness and crystallinity. Singh et al. (2025) enhanced paddy straw composites with SiO₂/C nanoparticles, achieving a 69.9% increase in specific strength at 0.4 wt% loading. Similarly, Rajaram et al. (2024) reported optimal mechanical properties in PLA composites reinforced with 40 wt% Tamarindus fruit fiber. These studies underscore how agro-waste and nano-reinforcements can produce high-performance, eco-friendly composites.

Further investigations by Kumar et al. (2022), Kocak et al. (2023), and Liu et al. (2024) have demonstrated that the incorporation of alkali-treated natural fillers such as cotton straw, rice husk, and corncob particles enhances not only mechanical performance but also water resistance and tribological behavior. Furthermore, Elgamsy et al. (2022) developed flame-retardant polyethylene composites using fibers such as jute, bagasse, and corn silk, showcasing the multifunctional potential of agricultural waste.

In this context, biomass from trees like *Ficus religiosa* (Peepal) and *Azadirachta indica* (Neem), which are frequently pruned in urban and rural landscapes, remains underutilized. Rather than discarding this biomass through incineration or composting, its lignocellulosic fiber structure offers a valuable opportunity for conversion into reinforcing agents for composites. Neem, in particular, is known for its bio-functional potential, including antimicrobial and insecticidal properties due to its rich phytochemical profile (Farhan et al., 2024; Ghaffar et al., 2024). Such features could further benefit the environmental resilience of the resulting composites. Neem is also known for insecticidal properties, which can be further enhanced by incorporating nanoparticle-based strategies for pest resistance (Gorge and Abood, 2025). The bio-functional properties of Neem-based composites could extend to environmental applications (Salman et al., 2024).

To improve interfacial bonding and mechanical integrity, silica nanoparticles (SiO_2) have been incorporated into polymer matrices. For instance, Long et al. (2022) demonstrated that epoxy adhesives modified with active-group-functionalized SiO_2 nanoparticles achieved up to 47.6% higher tensile strength and 62% greater flexural strength compared to unmodified adhesives. Similarly, Ben et al. (2024) utilized a polydopamine (PDA) surface treatment in combination with epoxy-grafted SiO_2 nanoparticles on UHMWPE fibers, resulting in a more than 2.5-fold increase in interfacial shear strength (from 2.47 MPa to 6.08 MPa).

Studies have shown their role in enhancing matrix–fiber interactions and mitigating environmental stress conditions (Maryam et al., 2025). These enhancements are critical for developing composites exposed to moisture or mechanical loads. Studies have shown that nanoformulations improve plant stress resilience (Hamzah and Ibrahim, 2024).

This study aims to develop hybrid epoxy composites reinforced with Neem and Peepal fibers along with silica nanoparticles. The novelty lies in the dual valorization approach—utilizing underexploited municipal tree waste and integrating functional nanofillers—to engineer high-performance, moisture-resistant green composites. Unlike previous works focused predominantly on agricultural residues, this research explores the untapped potential of urban tree biomass. The resulting composites are intended for sustainable applications in automotive interiors, packaging, and construction materials, aligning with circular economy goals and advancing the reuse of organic waste in high-value material systems.

2. Materials and Methods

2.1 Materials

The primary matrix material used in this study was a commercial-grade epoxy resin (LY556) and corresponding hardener (HY951), procured from a local supplier. Waste fibers from Peepal (*Ficus religiosa*) and Neem (*Azadirachta indica*) trees were collected from roadside pruning and municipal garden trimmings. The fibers were separated manually and cut into uniform lengths (20–30 mm). Analytical-grade silica (SiO_2) nanoparticles, with an average particle size of 30–50 nm and a purity of >99%, were sourced from Sigma-Aldrich for nanoparticle reinforcement. The properties of Peepal and Neem fibers are shown in Table 1. The characteristic of SiO_2 is shown in Table 2.

<Table 1 Properties of Peepal and Neem fibers>

<Table 2 characteristic of SiO_2 >

2.2 Fiber Treatment

To enhance fiber-matrix adhesion and remove surface impurities, the Peepal and Neem fibers underwent alkaline treatment. The fibers were soaked in a 5 wt% sodium hydroxide (NaOH) solution for 4 hours at room temperature, then washed thoroughly with distilled water until neutral pH was achieved. The treated fibers were dried in a hot air oven at 60°C for 24 hours and stored in moisture-proof containers until use.

2.3 Composite Fabrication

A hand lay-up method followed by compression molding was employed for composite fabrication. Table 3 shows the composite formulation details. Epoxy resin and hardener were mixed in a 10:1 ratio by weight, as recommended by the supplier. Silica nanoparticles were ultrasonicated in the epoxy resin for 30 minutes to ensure uniform dispersion. The treated Peepal

and Neem fibers were then introduced into the nanoparticle-loaded epoxy matrix at varying fiber volume fractions (10%, 20%, and 30%). The mixture was poured into a pre-cleaned mold and compressed under 10 MPa for 24 hours at room temperature to ensure proper curing. Post-curing was done at 80°C for 2 hours to enhance cross-linking.

<Table 3 Composite formulation>

2.4 Mechanical Testing

The mechanical behavior of the epoxy composites reinforced with treated Peepal and Neem fibers, along with silica nanoparticles, was evaluated using three standard tests: tensile, flexural, and impact. These tests provide a comprehensive understanding of the material's strength, stiffness, and resistance to sudden loads. All specimens were prepared and tested in accordance with ASTM standards.

2.4.1 Tensile test

The test was conducted by following ASTM D638 standard using a Universal Testing Machine (UTM) with a load capacity of 10 kN. The crosshead speed was maintained at 2 mm/min. Each composite variant was tested with at least five replicates to ensure statistical significance. Dog-bone-shaped specimens with a gauge length of 50 mm, overall length of 165 mm, and width of 13 mm were used.

2.4.2 Flexural test

A three-point bending setup was used on the UTM with a support span of 100 mm and a crosshead speed of 2 mm/min by following ASTM D790. The specimens were placed

horizontally on two supports, and load was applied at the center until fracture or significant deflection occurred. Rectangular specimen with dimensions 125 mm \times 12.5 mm \times 3 mm were used for three-point bending tests.

2.4.3 Impact test

The Izod impact test was conducted using a pendulum-type impact tester as per ASTM D256 standard. The specimen was vertically clamped with the notch facing the striking edge. The pendulum was released to strike the specimen, and the energy absorbed during fracture was recorded directly by the machine. Notched specimens with dimensions 65 mm \times 12.7 mm \times 3.2 mm were used.

2.4.4 Shore d hardness test

A Shore D durometer was used to test the hardness of the composite samples. Each specimen had dimensions of approximately 50 mm \times 50 mm \times 5 mm. The hardness was measured by pressing the indenter against the surface of the specimen under a consistent load and reading the dial after a dwell time of 15 seconds. Measurements were taken at five different points on each specimen, and the average value was reported.

2.5 Moisture Absorption Test

Moisture absorption behavior was studied as per ASTM D570. Composite specimens were oven-dried at 80°C for 24 hours, weighed (W_0), and then immersed in distilled water at room temperature. Specimens were removed at 24-hour intervals, surface-dried, and reweighed (W_1). The percentage of water absorption was calculated using:

$$\text{Moisture absorption (\%)} = [(W_1 - W_0) / W_0] \times 100$$

The test was continued until the samples reached saturation.

2.6 Density and void

The density of the composite was measured using the water displacement method (Archimedes principle). A digital balance with a density measurement kit was used. Each specimen was weighed in air (W_1) and in distilled water (W_2). The experimental density (ρ_e) was calculated using:

$$\rho_e = W_1 / (W_1 - W_2) \times \rho_{\text{water}}$$

Where ρ_{water} is the density of distilled water (0.997 g/cm³ at room temperature).

Theoretical density (ρ_t) was calculated using the rule of mixtures:

$$\rho_t = (W_f \times \rho_f + W_m \times \rho_m)$$

Where, W_f and W_m are the weight fractions of fiber and matrix; ρ_f and ρ_m are the densities of fiber and matrix, respectively

$$\text{Void content (\%)} = [(\rho_t - \rho_e) / \rho_t] \times 100$$

2.7 Morphological Analysis

The fracture surfaces of selected specimens were examined using SEM to observe the fiber–matrix interaction, nanoparticle dispersion, and void formation. Samples were gold-coated before analysis to prevent charging.

2.8 Data analysis

All mechanical property tests were conducted with five replicates per group, and results are reported as mean \pm standard deviation (SD). Statistical significance of performance differences among composite configurations was evaluated using one-way ANOVA in SPSS (v25) with a significance level of $\alpha = 0.05$. When ANOVA indicated significant variation, Tukey's Honestly Significant Difference (HSD) post-hoc test was applied to determine specific group differences at the 95% confidence level.

3. Results and discussion

3.1 Tensile strength

<Figure 1 Tensile strength variation in epoxy composites with peepal-neem hybrid fibers fortified with silica>

Figure 1 illustrates the tensile behavior of epoxy/peepal/neem/silica composite. Neat epoxy exhibited the lowest strength (40 MPa), reflecting its brittle thermoset nature and absence of reinforcing phases. With the incorporation of lignocellulosic fibres, tensile strength increased substantially due to axial load transfer and crack arresting mechanisms imparted by the fibres (Akter et al., 2024). Notably, stacking sequence played a crucial role in governing fibre–matrix interaction and stress distribution. The N/P/N (Neem–Peepal–Neem) configuration attained 60 MPa, whereas the P/N/P arrangement showed only 48 MPa. This superior performance of N/P/N was attributed to the higher lignin and cellulose contents of Neem fibres in the outer layers, which improved interfacial bonding, resisted fibre pull-out, and offered better compatibility with the epoxy matrix compared to the more hydrophilic Peepal fibres.

Further enhancement was observed with silica nanoparticle incorporation into the optimal N/P/N stacking. Introduction of 1 wt% SiO₂ increased the strength to 66 MPa, and the peak strength of 70 MPa was achieved at 2 wt% loading. The improvement arose from nanosilica's high surface area, which promoted mechanical interlocking with polymer chains, bridged microvoids, and pins crack tips—thereby increased resistance to tensile deformation (Singh et al., 2021). However, a slight decline at 3 wt% (67 MPa) indicated the onset of nanoparticle agglomeration, which can act as stress concentration sites, inhibited stress transfer, and led to premature failure.

<Table 4 Comparative analysis of mechanical properties of hybrid natural fiber-reinforced composites with nanoparticles additives>

The tensile performance of the developed composites was also compared with other reported hybrid natural fiber-reinforced polymer composites containing nanoparticle additives (Table 4). The Neem/Peepal/SiO₂ composite exhibited the highest tensile strength of 70 MPa (N/P/N + 2 wt % SiO₂), which was substantially higher than hemp/sisal/SiO₂ composites (48 MPa, Singh et al., 2021), jute/flax/graphene laminates (51 MPa, Venkatesh et al., 2023), and kenaf/pineapple/graphene composites (20 MPa, Dhilipkumar et al., 2025). These results confirmed that the combination of Neem fibers in the outer layers, Peepal fibers in the core, and well-dispersed nanosilica particles provided superior load-bearing capability through improved interfacial bonding, enhanced stress transfer, and micro-void bridging.

Statistical analysis confirmed that the differences among composite configurations were highly significant (one-way ANOVA, $p = 2.8 \times 10^{-17}$, $F = 102.4$). Tukey's HSD post-hoc test

showed that the N/P/N + 2 wt% SiO₂ composite had a significantly higher tensile strength ($p < 0.05$) than all other groups (Table 5).

<Table 5 Statistical summary of tensile strength>

3.2 Flexural strength

<Figure 2 Flexural strength variation in epoxy composites with peepal-neem hybrid fibers fortified with silica>

Figure 2 shows flexural strength consequence of epoxy/peepal/neem/silica composite. . Neat epoxy exhibited the weakest bending performance (45 MPa) due to brittle fracture and lack of reinforcement mechanisms. Upon the introduction of lignocellulosic fibres, the bending resistance increased appreciably because fibres were able to bridge cracks and resisted tensile stresses generated on the outer surface during bending (Nampoothiri et al. 2022). Between the two hybrid sequences, the Peepal-dominant P/N/P sample displayed a moderate strength of 52 MPa, whereas the Neem-dominant N/P/N configuration reached 65 MPa. This improvement was attributed to Neem fibres possessing higher tensile modulus and cellulose content, which aided in restraining deformation and maintaining structural rigidity under flexural stresses (Ramesh et al. 2017). Additionally, better interfacial adhesion and reduced moisture-induced swelling in Neem layers favour increased fibre-matrix compatibility compared to Peepal.

Incorporating silica nanoparticles into the N/P/N configuration further enhanced flexural strength due to nano-scale reinforcement and crack-bridging effects. At 1 wt% SiO₂, the strength improved to 70 MPa, while at 2 wt% the maximum of 74 MPa was achieved. Mechanistically, well-dispersed nanosilica particles occupied voids, promoted homogeneous stress transfer,

enhanced stiffness, and impeded crack propagation (Singh et al. 2021). However, at 3 wt% SiO₂, a marginal decline to 71 MPa suggested that particle agglomeration introduced stress raisers and micro-defects, led to earlier crack initiation under bending loads.

As shown in Table 4, the flexural strength of 74 MPa for the Neem/Peepal/SiO₂ composite was higher than that of hemp/sisal/SiO₂ (50 MPa, Singh et al., 2021) and jute/flax/graphene laminates (55 MPa, Venkatesh et al., 2023), but lower than coir/basalt/TiC hybrid composites (200 MPa, Arshad et al., 2021) due to the extremely rigid basalt fibers and hard ceramic reinforcement used in the latter system. This positioned the present laminate as mechanically superior to typical lignocellulosic hybrids while maintaining a more sustainable and lower-density profile as fiber/particle systems optimized purely for stiffness.

The performance variations were statistically significant (one-way ANOVA, $p = 6.5 \times 10^{-19}$, $F = 118.6$). Post-hoc analysis confirmed that the N/P/N + 2 wt% SiO₂ laminate exhibited flexural strength values significantly greater than those of other stacking sequences and filler loadings ($p < 0.05$) (Table 6).

<Table 6 Statistical summary flexural strength>

3.3 Impact strength

<Figure 3 Impact strength variation in epoxy composites with peepal-neem hybrid fibers fortified with silica>

Figure 3 illustrates impact strength consequence of epoxy/peepal/neem/silica composite. Neat epoxy displayed very poor impact strength (2.5 kJ/m^2), characteristic of its inherently brittle nature and lack of energy-absorbing mechanisms during crack initiation or propagation. With the incorporation of lignocellulosic fibres, the composites exhibited enhanced toughness owing to a variety of energy-dissipating mechanisms such as microcrack deflection, fibre pull-out, and fibre bridging (Venkatesh et al., 2023). Among the hybrid lay-ups, the P/N/P configuration provided moderate improvement (3.2 kJ/m^2), whereas the N/P/N design achieved a higher value of 4.0 kJ/m^2 . This difference highlights the relatively greater ductility, higher tensile strain-to-failure and improved interfacial bonding characteristics of Neem fibres, which enabled them to absorb and dissipate greater amounts of impact energy compared to Peepal fibres.

Further enhancements were noted when SiO_2 nanoparticles were incorporated into the N/P/N fibre structure. At 1 wt%, an impact strength of 4.5 kJ/m^2 was achieved, primarily due to crack-pinning by well-dispersed nanosilica, matrix toughening through plastic zone enlargement, and reduction of voids between fibres and matrix. The optimum performance occurred at 2 wt% SiO_2 , where the impact resistance reached 5.0 kJ/m^2 . The combined macro-reinforcement of fibres and micro-scale crack tip blunting effect of nanosilica created a synergistic toughening response. However, at 3 wt% SiO_2 , a small decline (to 4.6 kJ/m^2) was observed. This was attributed to particle agglomeration acting as micro-notches, which served as stress concentrators and facilitate brittle failure (Sinha et al. 2020).

The impact strength differences among all configurations were highly significant (one-way ANOVA, $p = 1.2 \times 10^{-16}$, $F = 91.8$). Tukey's test indicated that the N/P/N + 2 wt% SiO₂ composite outperformed all other variants with a statistically significant margin ($p < 0.05$) (Table 7).

<Table 7 Statistical summary impact strength>

3.4 Hardness

<Figure 4 Hardness variation in epoxy composites with peepal-neem hybrid fibers fortified with silica>

Figure 4 depicts the variation in Shore-D hardness of epoxy/peepal/neem/silica composite. . Neat epoxy exhibited the lowest hardness (55 Shore D), reflecting the relatively compliant nature of the polymer surface in the absence of rigid reinforcements. Upon introducing natural fibres, noticeable improvements were observed due to increased resistance to surface indentation stemming from the stiff lignocellulosic reinforcement phase. The P/N/P configuration achieved a hardness of 60 Shore D, while the Neem-dominated N/P/N assembly displayed a higher value of 65 Shore D. This superior performance was attributed to the greater inherent stiffness and higher lignin content of Neem fibres, which enhanced fibre-matrix mechanical interlocking, reduced localised deformation, and limited plastic movement under the applied load of the durometer indenter.

Further enhancement in hardness was obtained with the incorporation of nanosilica into the N/P/N laminate structure (Iskakov et al., 2025; Kademane et al., 2024). At 1 wt% SiO₂,

hardness increased to 68 Shore D, indicating that nanoscale fillers effectively occupied microvoids within the matrix and fibre-matrix interface, thus constrained polymer chain mobility and resisted surface deformation. The highest surface hardness (70 Shore D) was reached at 2 wt% SiO₂ loading. This peak was attributed to the synergistic reinforcing effect of macro-scale natural fibres and micro-scale silica nanoparticles that improved stiffness, induced strain hardening, and promoted uniform stress distribution across the composite surface. However, a slight decline to 69 Shore D was observed at 3 wt% silica, signifying a threshold beyond which further addition might lead to agglomeration and interference with homogeneous reinforcement—thereby reduced the overall effectiveness in resisting surface indentation.

Hardness values showed statistically significant variation across all composite groups (one-way ANOVA, $p = 4.7 \times 10^{-15}$, $F = 78.3$). Post-hoc comparisons identified the N/P/N + 2 wt% SiO₂ laminate as having a significantly higher Shore D hardness than all other configurations ($p < 0.05$) (Table 8).

<Table 8 Statistical summary Shore D Hardness>

3.5 Water absorption

<Figure 5 Water absorption variations in epoxy composites with peepal-neem hybrid fibers fortified with silica>

Figure 5 illustrates the water absorption profiles of epoxy/peepal/neem/silica composite over a 12-day immersion period. Due to the presence of hydrophilic hydroxyl groups in natural

fibres, all reinforced composites displayed higher water uptake relative to neat epoxy. However, substantial differences were observed based on fibre type and nanosilica loading. The P/N/P laminate exhibited the highest equilibrium absorption (85%), which can be attributed to the higher hemicellulose and moisture content of Peepal fibres, led to greater fibre swelling and micro-cracking at the fibre–matrix interface. This swelling promoted capillary action and facilitated water migration into the composite interior. In contrast, the Neem-rich N/P/N configuration showed a significantly lower saturation level (70%), indicated that Neem fibres, with their lower hydrophilicity and superior interfacial compatibility, provided greater resistance to moisture ingress and associated debonding.

Incorporation of silica nanoparticles into the optimal N/P/N stacking further reduced the overall water absorption due to a combined barrier and void-blocking effect (Iskakov et al., 2025; Kademane et al., 2024). At 1 wt% SiO₂, water uptake decreased to 63% as nanoparticles occupied micro-voids. With an increase to 2 wt%, a further reduction (57%) was recorded, suggesting improved tortuosity of diffusion pathways and reduced permeability of the polymer network. The lowest water absorption (52%) was achieved at 3 wt%, signifying maximum hindrance to water diffusion as a result of nanoparticle densification within the matrix.

3.6 Density and void

<Figure 6(a) Density variation in epoxy composites with peepal-neem hybrid fibers fortified with silica>

Figure 6(a) shows the theoretical and experimental densities of epoxy/peepal/neem/silica composite. The neat epoxy matrix exhibited a theoretical density of 1.20 g/cm³, whereas the experimental value was slightly lower (1.18 g/cm³), suggested negligible voids and effective

curing under the employed processing conditions. Upon incorporation of natural fibres, theoretical densities increased due to the relatively higher densities of Neem and Peepal fibres compared to the epoxy matrix. The P/N/P laminate displayed a theoretical density of 1.22 g/cm³, marginally higher than the N/P/N configuration, which was consistent with the higher bulk density of Peepal fibres. However, the corresponding experimental values remained lower than theoretical estimates across both stacking sequences, indicating partial infiltration of resin into fibre bundles and presence of micro-voids—phenomena commonly associated with lay-up processing of natural-fibre composites.

Introduction of SiO₂ nanoparticles into the N/P/N composite progressively enhanced both theoretical and experimental densities. As the theoretical density increased from 1.21 g/cm³ (1 wt% SiO₂) to 1.225 g/cm³ (3 wt% SiO₂), the experimental density concurrently rose from 1.195 g/cm³ to 1.21 g/cm³. This increase reflected the relatively high intrinsic density of silica nanoparticles (2.2 g/cm³) and their efficient dispersion within the matrix. Crucially, the narrowing gap between theoretical and experimental densities with increasing silica content indicated improved packing efficiency, reduced micro-void formation, and enhanced infiltration of the epoxy resin around fibres. The densification effect resulted from nanoparticles filling microscopic defects and interstitial spaces, thereby improved matrix continuity.

<Figure 6(b) Void variation in epoxy composites with peepal-neem hybrid fibers fortified with silica>

Figure 6(b) depicts the variation of void content of epoxy/peepal/neem/silica composite. Void formation is a critical defect that can significantly impair mechanical strength, moisture resistance, and long-term stability. The neat epoxy exhibited the lowest void content (1.25 %),

confirming efficient resin curing with minimal entrapped air or micro-porosity due to the absence of reinforcing phases. However, upon incorporation of natural fibres, void content marginally increased to 1.55–1.57 % in both P/N/P and N/P/N sequences. This increase was attributed to the hygroscopic and porous character of lignocellulosic fibres which tend to retain moisture, swell, and resist complete resin impregnation, particularly during hand lay-up processing. In addition, gaps between fibre bundles and matrix compound the likelihood of trapped air pockets.

The influence of SiO₂ nanoparticles on void content within the N/P/N stacking sequence exhibited a non-linear trend. Introducing 1 wt% SiO₂ resulted in a slight rise in voids (1.65 %), likely due to nanoparticle agglomeration causing localised resin flow interruption and trapping air pockets during curing. However, increasing the nanoparticle content to 2 wt% led to a decrease in voids to 1.48 %, and a further decline to 1.32 % was achieved at 3 wt% loading. The reduction in void formation at higher nanoparticle contents suggested improved resin flowability and filler-matrix compatibility, whereby well-dispersed nanosilica filled micro-channels between fibres and matrix, eliminated potential nucleation sites for voids.

3.7 Fracture surface analysis

<Figure 7 Micrographs of broken samples (a) N/P/N + 2wt% SiO₂ (b) N/P/N + 3wt% SiO₂>

Figure 7 presents SEM micrographs of the fracture surfaces of N/P/N + 2wt% SiO₂ and N/P/N + 3wt% SiO₂ composites.

In Figure 7(a), the fracture surface of the N/P/N + 2 wt% SiO₂ composite displays relatively uniform fiber dispersion and strong fiber–matrix interfacial bonding, as evidenced by

fewer fiber pull-outs and cleaner matrix adherence. This correlates with the optimal mechanical performance observed for this composition, indicating efficient stress transfer and minimal void content.

In contrast, Figure 7(b), corresponding to the N/P/N + 3 wt% SiO₂ composite, reveals localized regions of nanoparticle agglomeration and minor void formation. Although fiber–matrix adhesion is still evident, there is a slight increase in fiber pull-out and rougher surface morphology compared to the 2 wt% sample. This suggests that excessive nanoparticle loading may hinder uniform dispersion, leading to localized stress concentrations and marginal reductions in mechanical performance. These microstructural observations support the conclusion that 2 wt% SiO₂ provides the most favorable balance between reinforcement and matrix compatibility.

Preliminary estimation based on SEM images indicates that the pore (void) size in the fractured matrix ranges between 4–6 µm. The fiber pull-out lengths were found to be in the range of 100–200 µm, with reduced pull-out lengths observed in the 2 wt% SiO₂ composite, suggesting enhanced fiber–matrix bonding.

3.8 Environmental significance:

The environmental benefits of the developed composites arise from both material selection and improved performance. Using Neem and Peepal fibers—urban biomass waste typically incinerated or landfilled—reduces raw material consumption and avoids CO₂ and CH₄ emissions from open burning, similar to other waste-valorization approaches (Prasad et al., 2024; Santhosh et al., 2024). Incorporation of silica nanoparticles enhanced tensile, flexural, and moisture-resistance properties, extending service life and reducing replacement frequency. This

durability-related advantage aligns with findings in other silica-reinforced biocomposites, where improved matrix integrity minimized material wastage (Iskakov et al., 2025; Kademane et al., 2024).

Nanoformulations are also being applied as edible coatings and nanoemulsions to extend product shelf life and enhance surface functionality (Wang et al., 2025), while green synthesis approaches support sustainability goals (Naz et al., 2025). Approximately 30 wt % of the composite content originated from biomass waste. Benchmarking against agricultural-waste composites (Liu et al., 2024; Kumar and Saha, 2022) suggests that such substitution could measurably lower environmental impact. Although a full life cycle assessment was not performed, these indicators highlight how combining underutilized fibers with nanosilica supports circular-economy principles by promoting renewable raw materials, reducing waste, and lowering the overall environmental burden.

4. Conclusion

This study explored the development of hybrid epoxy composites reinforced with Neem and Peepal tree waste fibers along with silica (SiO_2) nanoparticles. The key findings are summarized below:

- Composites were successfully fabricated using hand lay-up and compression molding techniques, incorporating different stacking sequences (N/P/N and P/N/P) and SiO_2 loadings (1–3 wt%).
- The N/P/N stacking sequence demonstrated superior mechanical performance compared to P/N/P. The composite with N/P/N + 2 wt% SiO_2 exhibited the highest tensile strength

(70 MPa), flexural strength (74 MPa), impact strength (5.0 kJ/m²), and hardness (70 Shore D).

- A slight decline in mechanical properties was observed at 3 wt% SiO₂, attributed to nanoparticle agglomeration causing stress concentration zones.
- Water absorption was significantly reduced with increased SiO₂ content, reaching the lowest value (52%) in the N/P/N + 3 wt% SiO₂ composite due to enhanced barrier effects and void filling by the nanoparticles.
- The void content decreased from 1.65% to 1.32%, and the experimental densities closely matched theoretical values as silica content increased, confirming better matrix packing and reduced porosity.
- Overall, the N/P/N + 2 wt% SiO₂ composite formulation offered the most balanced performance in terms of strength, moisture resistance, and structural integrity.
- This research demonstrates a sustainable approach to converting urban biomass waste into high-performance composite materials, aligning with circular economy principles and offering potential for structural, automotive, and eco-friendly packaging applications.

Ethics approval

This material is the authors' own original work, which has not been previously published elsewhere. The paper is not currently being considered for publication elsewhere. All authors have been personally and actively involved in substantial work leading to the paper, and will take public responsibility for its content.

Funding

No funding received from any funding resources

Conflicts of interest

The authors have no conflicts of interest to declare. All co-authors have seen and agree with the contents of the manuscript and there is no financial interest to report. We certify that the submission is original work and is not under review at any other publication

References

Akter, M., Uddin, M.H. and Anik, H.R. (2024). Plant fiber-reinforced polymer composites: a review on modification, fabrication, properties, and applications. *Polymer Bulletin*, **81**(1), 1–85.

Arshad, M.N., Mohit, H., Sanjay, M.R., Siengchin, S., Khan, A., Alotaibi, M.M., Asiri, A.M. and Rub, M.A. (2021). Effect of coir fiber and TiC nanoparticles on basalt fiber reinforced epoxy hybrid composites: physico–mechanical characteristics. *Cellulose*, **28**, 3451–3471.

Ben, N., Jiang, S., Zhao, L., Gong, J., Shen, L., Wang, K. and Tang, C., 2025. Enhancing the interfacial property between UHMWPE fibers and epoxy through polydopamine and SiO₂ surface modification. *ChemistryOpen*, *14*(1), p.e202400131.

Dhilipkumar, T., Arunpandian, M., Arumugam, S., Sadeq, A.M., P, K., Oh, T.H., Bahajjaj, A.A.A., Shankar, K.V. and Selvakumar, K. (2025). Exploring the synergistic effects of graphene on the mechanical and vibrational response of kenaf/pineapple fiber-reinforced hybrid composites. *Polymer Composites*, **46**(5), 4591–4604.

Elgamsy, R., Khalid, I., Taha, N., Sadek, S., Tawfic, M.L., Attia, T. and Elsabbagh, A. (2022). Developing fire retardant composites of biodegradable polyethylene reinforced with agricultural wastes. *Ain Shams Engineering Journal*, **13**(6), 101768.

Eyupoglu, S., Eyupoglu, C. and Merdan, N. (2025). Characterization of a novel natural plant-based fiber from reddish shell bean as a potential reinforcement in bio-composites. *Biomass Conversion and Biorefinery*, **15**(3), 4259–4268.

Farhan, M., Akhtar, S., Ahmad, I., Maryam, Hussain, H., Yasin, M., Farooqi, M.A. and Zhang, S. (2024). Assessing the potential of nano-formulated chlorfenapyr and clothianidin insecticides-treated sugar baits against *Anopheles funestus*, *Anopheles coluzzii* and *Culex quinquefasciatus* mosquitoes. *Acta Tropica*, **256**, 107269.

Ghaffar, S., Niaz, H., Amjad, M.U. and Rizwan, M. (2024). Morphological responses of zinnia (*Zinnia elegans* L.) to foliar application of neem extract. *Journal of Horticultural Science and Technology*, **7**(2), 52–57.

Gorge, W.A. and Abood, M.F. (2025). Magnesium oxide nanoparticles synthesized from *Solanum elaeagnifolium* and their effect against mealybugs *Phenacoccus solenopsis* Tinsley. *Journal of Global Innovations in Agricultural Sciences*, 391–395. <https://doi.org/10.22194/jgias/25.1306>

Hamzah, L.M. and Ibrahim, M. (2024). Optimizing sour orange growth and chemical properties through foliar application of nano and organic fertilizers. *Journal of Global Innovations in Agricultural Sciences*, 709–715. <https://doi.org/10.22194/jgias/24.1303>

Iskakov, R.M., Bukanova, A.S., Kalauova, A.S., Kairliyeva, F.B., Nauashev, A.N., Shambilova, G.K., Obidin, I.M., Kuzin, M.S., Chernenko, D.N., Patsaev, T.D. and Gerasimenko, P.S. (2025).

Eco-Friendly Polypropylene Composites Reinforced with Cellulose Fibers and Silica Nanoparticles. *Polymers*, **17**(10), 1290.

Kademane, A., Sur, S., Bagaria, O., Shashikala, A.R., Venkatesh, R., De Pours, M.V., Christysudha, J., Seikh, A.H. and Iqbal, A. (2024). Synthesis and characterization study of Roselle fiber bonded polypropylene composite enriched by silica nanoparticles derived from bryophyllum pinnatum leaf waste. *Biomass Conversion and Biorefinery*, **14**(24), 31009–31019.

Kocak, E.D., Olcay, H. and Yildiz, Z. (2023). Mechanical and acoustic properties of alkali treated agricultural waste reinforced sustainable polyurethane composites. *Journal of Reinforced Plastics and Composites*, **42**(21–22), 1191–1203.

Kumar, S. and Saha, A. (2022). Effects of particle size on structural, physical, mechanical and tribology behaviour of agricultural waste (corn cob micro/nano-filler) based epoxy biocomposites. *Journal of Material Cycles and Waste Management*, **24**(6), 2527–2544.

Liu, Y., Ou, M., Gao, Y., Ding, H., Zhuo, L. and Ma, Y. (2024). Development and characterization of polymer composites with cotton straw fiber derived from agricultural wastes. *Polymer Composites*, **45**(17), 16304–16316.

Long, J., Li, C. and Li, Y., 2022. Enhancement of mechanical and bond properties of epoxy adhesives modified by SiO₂ nanoparticles with active groups. *Polymers*, **14**(10), p.2052.

Maryam, El-Mogy, M.M., Jan, M.F., Naz, I., Ahmad, I., Ahmad, R. and Altaf, M.T. (2025). Nanoparticle Innovations for Mitigating Metal Toxicity in Plants. *Phyton*, **94**(3), 623–640.

Nampoothiri, E.N., Bensam Raj, J., Thanigaivelan, R. and Karuppasamy, R., 2022. Experimental investigation on mechanical and biodegradation properties of indian almond–kenaf fiber-

reinforced hybrid composites for construction applications. *Journal of Natural Fibers*, 19(1), pp.292-302.

Naz,I., Maryam, Chahel,A.A., Ahmad,I., Raza,A., Haider,M.W., Zaheer,M.S., Riaz,M.W., Rizwan,M. and Manoharadas,S. (2025). Investigating the use of green synthesized copper oxide nanoparticles from *Melia azedarach* to combat cadmium stress in wheat. *Scientific Reports*, 15(1). <https://doi.org/10.1038/s41598-025-10168-x>

Prasad, V., Alliyankal Vijayakumar, A., Jose, T. and George, S.C., 2024. A comprehensive review of sustainability in natural-fiber-reinforced polymers. *Sustainability*, 16(3), p.1223.

Rajaram, S., Subbiah, T., Arockiasamy, F.S. and Iyyadurai, J. (2024). Transforming agricultural waste into sustainable composite materials: Mechanical properties of tamarindus fruit fiber (TFF)-reinforced polylactic acid composites. *Engineering Proceedings*, 61(1), 32.

Ramesh, M., Deepa, C., Aswin, U.S., Eashwar, H., Mahadevan, B. and Murugan, D., 2017. Effect of alkalization on mechanical and moisture absorption properties of Azadirachta indica (neem tree) fiber reinforced green composites. *Transactions of the Indian Institute of Metals*, 70(1), pp.187-199.

Salman,R.A., Alzubaidy,M.W.M. and Tawfeeq,A.T. (2024). Effect of *Mirabilis jalapa* plant fortified with nano-quercetin to accelerate wound healing in vivo. *Journal of Global Innovations in Agricultural Sciences*, 717–723. <https://doi.org/10.22194/jgias/24.1450>

Santhosh, N., Praveena, B.A., Gowda, A.C., Duhduh, A.A., Rajhi, A.A., Alamri, S., Berwal, P., Khan, M.A. and Wodajo, A.W., 2024. Innovative eco-friendly bio-composites: A comprehensive

review of the fabrication, characterization, and applications. *Reviews on Advanced Materials Science*, 63(1), p.20240057.

Sathish, M., Radhika, N., Venuvanka, N. and Rajeshkumar, L. (2024). A review on sustainable properties of plant fiber-reinforced polymer composites: characteristics and properties. *Polymer International*, 73(11), 887–943.

Şen, İ. and Sever, K. (2025). Production and characterization of agricultural waste natural fiber-filled polylactic acid composites. *Polymer Bulletin*, 82(9), 4051–4074.

Singh, J., Gupta, A., Singh, M. and Saini, J. (2025). Influence of SiO₂/C nanoparticles on specific strength and stiffness in agro-waste reinforced polymer composites: experimental and numerical investigations. *Physica Scripta*. 100(3), p.035935.

Singh, T., Gangil, B., Ranakoti, L. and Joshi, A. (2021). Effect of silica nanoparticles on physical, mechanical, and wear properties of natural fiber reinforced polymer composites. *Polymer Composites*, 42(5), 2396–2407.

Sinha, R.K., Sridhar, K., Purohit, R. and Malviya, R.K., 2020. Effect of nano SiO₂ on properties of natural fiber reinforced epoxy hybrid composite: A review. *Materials Today: Proceedings*, 26, pp.3183-3186.

Venkatesh, R., Santhosh Kumar, P.C., Senthilkumar, A., Krishna, J.P., Chandramohan, P., Aneesh, V.N., Malladi, A., Priya, C.B. and Ramaraj, E. (2023). Mechanical Interlocking Approaches to the Prediction of Mechanical and Tribological Behavior of Natural Fiber-Reinforced Polymer Hybrid Nanocomposites or Automotive Applications. *Advances in Polymer Technology*, 2023(1), 6685060.

Wang,Y., Shaukat,M., Farhan,M. and Pan,J. (2025). Role of essential oil nanoemulsion and biopolymer-based edible coatings on postharvest quality preservation of fruits and vegetables during cold storage. *Journal of Horticultural Science and Technology*, 1–11.
<https://doi.org/10.46653/jhst25081001>

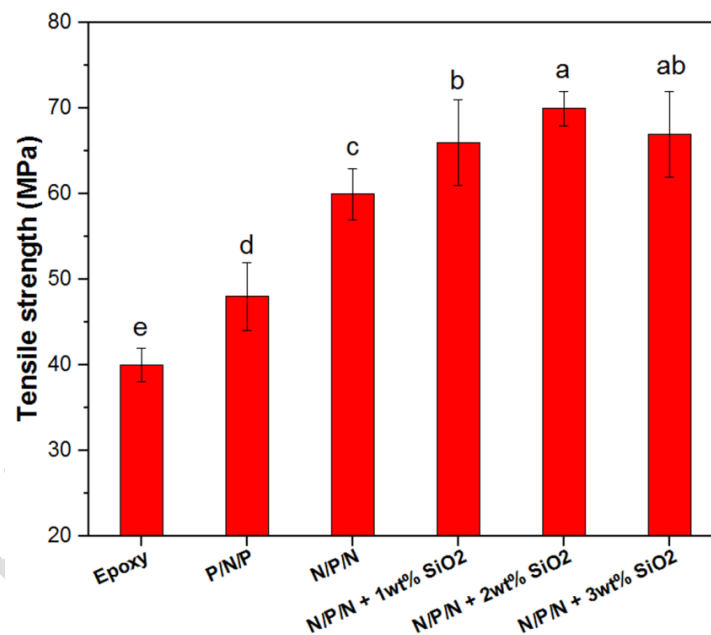


Figure 1 Tensile strength variation in epoxy composites with peepal-neem hybrid fibers fortified with silica

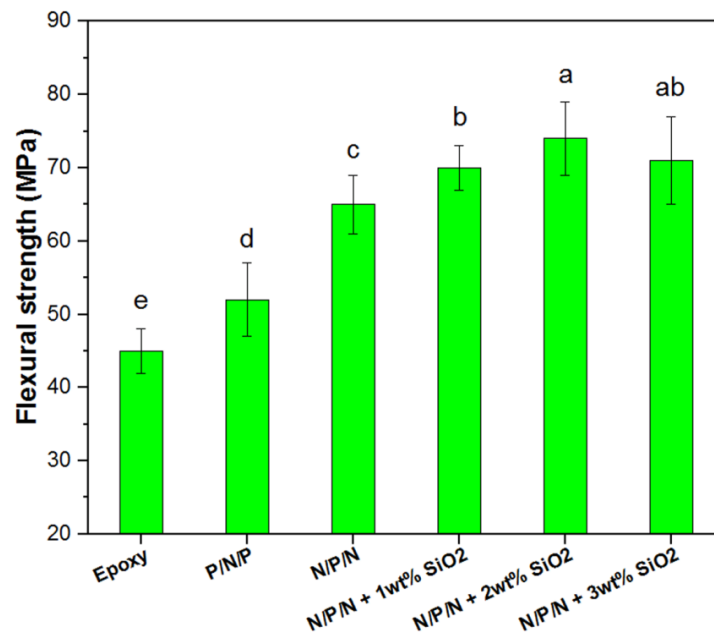


Figure 2 Flexural strength variation in epoxy composites with peepal-neem hybrid fibers fortified with silica

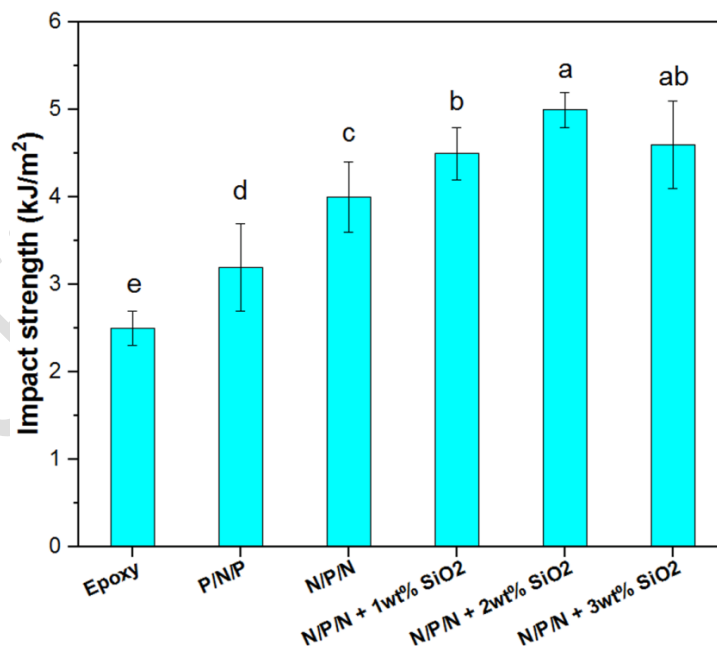


Figure 3 Impact strength variation in epoxy composites with peepal-neem hybrid fibers fortified with silica

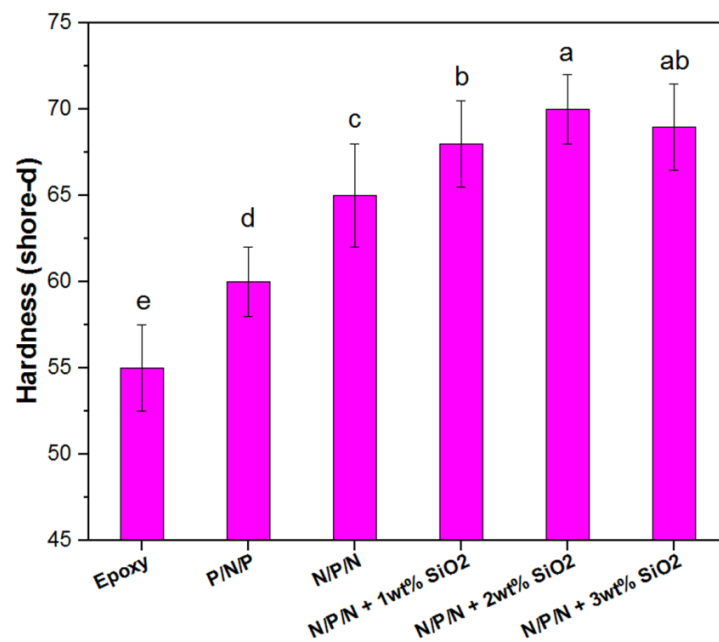


Figure 4 Hardness variation in epoxy composites with peepal-neem hybrid fibers fortified with silica

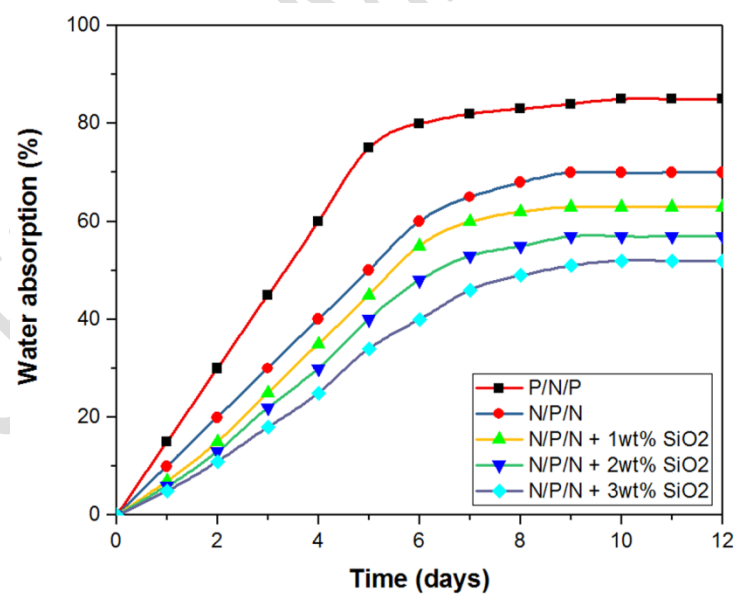


Figure 5 Water absorption variations in epoxy composites with peepal-neem hybrid fibers fortified with silica

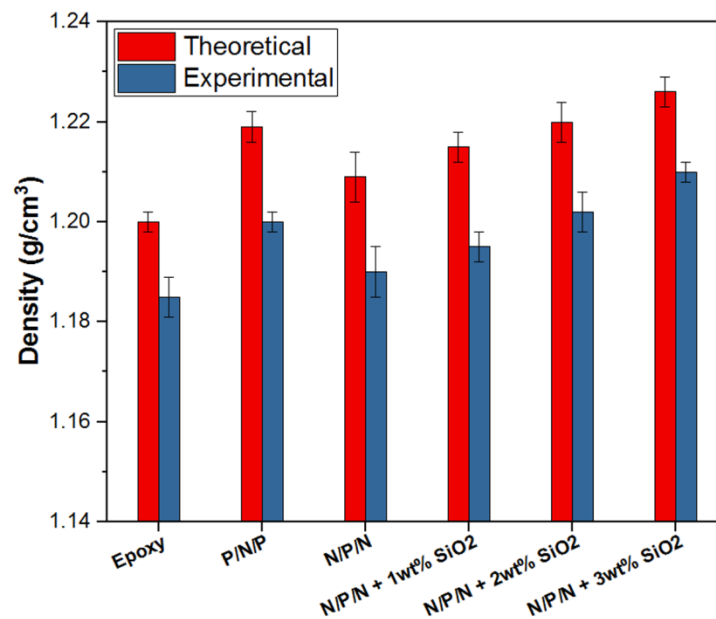


Figure 6(a) Density variation in epoxy composites with peepal-neem hybrid fibers fortified with silica

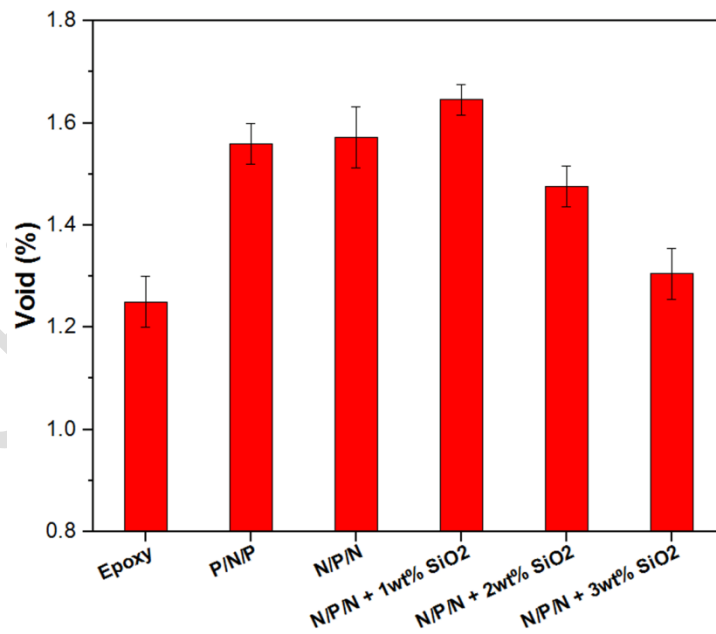


Figure 6(b) Void variation in epoxy composites with peepal-neem hybrid fibers fortified with silica

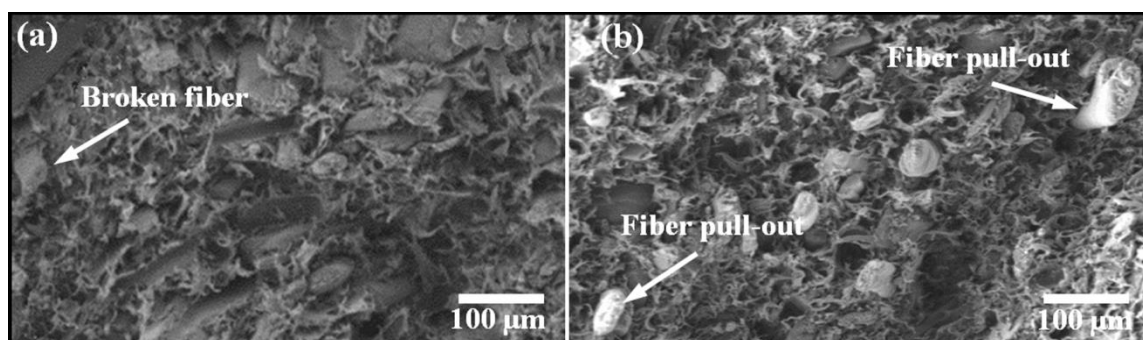


Figure 7 Micrographs of broken samples (a) N/P/N + 2wt% SiO₂ (b) N/P/N + 3wt% SiO₂

Table 1 Properties of Peepal and Neem fibers

Properties	Neem	Peepal
Cellulose	52 %	57%
Hemicelluloses	21%	19%
Lignin	16%	13%
Moisture	8%	9%
Density	1.2%	1.3%

Table 2 Characteristics of SiO₂

Properties	Values
Form	Powder
Purity	99.9%
Particle size	50 to 100 nm
Density	2.2 g/cm ³

Table 3 Composite formulation

Composites	Epoxy (wt%)	Peepal (wt%)	Neem (wt%)	SiO ₂ (wt%)
Epoxy	100	0	0	0
P/N/P	70	20	10	0
N/P/N	70	10	20	0
N/P/N + 1wt% SiO ₂	69	10	20	1
N/P/N + 2wt% SiO ₂	68	10	20	2
N/P/N + 3wt% SiO ₂	67	10	20	3

Table 4 Comparative analysis of mechanical properties of hybrid natural fiber-reinforced composites with nanoparticles additives

Composites	Tensile strength (MPa)	Flexural strength (MPa)	References
Neem/Peepal/SiO ₂	70	74	Current study
Coir/Basalt/TiC	58	200	Arshad et al. (2021)
Hemp/Sisal/SiO ₂	48	50	Singh et al. (2021)
Jute/Flax/Gr	51	55	Venkatesh et al. (2023)
Kenaf/Pineapple/Graphene	20	48	Dhilipkumar et al. (2025)

Table 5 Statistical summary of tensile strength

Composite	Mean \pm SD	95% CI
Epoxy	40.2 \pm 1.1	39.3 – 41.1
P/N/P	48.4 \pm 1.3	47.3 – 49.5
N/P/N	60.1 \pm 1.5	58.8 – 61.4
N/P/N + 1% SiO ₂	66.0 \pm 1.4	64.8 – 67.2
N/P/N + 2% SiO ₂	70.2 \pm 1.2	69.1 – 71.3
N/P/N + 3% SiO ₂	67.3 \pm 1.6	65.8 – 68.8

Table 6 Statistical summary flexural strength

Composite	Mean \pm SD	95% CI
Epoxy	45.3 \pm 1.2	44.2 – 46.4
P/N/P	52.6 \pm 1.4	51.4 – 53.8
N/P/N	64.8 \pm 1.5	63.5 – 66.1
N/P/N + 1% SiO ₂	70.1 \pm 1.3	69.0 – 71.2
N/P/N + 2% SiO ₂	74.0 \pm 1.1	73.0 – 75.0
N/P/N + 3% SiO ₂	71.2 \pm 1.4	70.0 – 72.4

Table 7 Statistical summary impact strength

Composite	Mean \pm SD	95% CI
Epoxy	2.6 \pm 0.1	2.5 – 2.7
P/N/P	3.2 \pm 0.2	3.0 – 3.4
N/P/N	4.0 \pm 0.2	3.8 – 4.2
N/P/N + 1% SiO ₂	4.5 \pm 0.2	4.3 – 4.7
N/P/N + 2% SiO ₂	5.0 \pm 0.1	4.9 – 5.1
N/P/N + 3% SiO ₂	4.6 \pm 0.2	4.4 – 4.8

Table 8 Statistical summary Shore D Hardness

Composite	Mean \pm SD	95% CI
Epoxy	55.2 \pm 1.1	54.3 – 56.1
P/N/P	60.4 \pm 1.0	59.6 – 61.2
N/P/N	65.1 \pm 1.0	64.3 – 65.9
N/P/N + 1% SiO ₂	68.0 \pm 0.9	67.2 – 68.8
N/P/N + 2% SiO ₂	70.3 \pm 1.0	69.5 – 71.1
N/P/N + 3% SiO ₂	69.1 \pm 1.1	68.2 – 70.0